Ribosomal protein S3 mediates drug resistance of proteasome inhibitor: potential therapeutic application in multiple myeloma

Gege Chen,[1]* Xuejie Gao,[1]* Xinyan Jia,[1] Yingcong Wang,[2] Li Xu,[1] Dandan Yu,[2] Shuaikang Chang,[1] Hui Deng,[1] Ke Hu,[1] Guanli Wang,[1] Bo Li,[3] Zhijian Xu,[3] Yumeng Lu,[2] Huaping Wang,[2] Ting Zhang,[2] Dongliang Song,[2] Guang Yang,[2] Xiaosong Wu,[2] Huabin Zhu,[2] Weiliang Zhu[3] and Jumei Shi[1]

[1]Department of Hematology, Shanghai East Hospital, Tongji University School of Medicine; [2]Department of Hematology, Shanghai Tenth People's Hospital, Tongji University School of Medicine and [3]CAS Key Laboratory of Receptor Research, State Key Laboratory of Drug Research, Drug Discovery and Design Center, Shanghai Institute of Materia Medica, Chinese Academy of Sciences, Shanghai, China

*GC and XG contributed equally as first authors.

Abstract

Multiple myeloma (MM) remains incurable due to drug resistance. Ribosomal protein S3 (RPS3) has been identified as a non-Rel subunit of NF-κB. However, the detailed biological roles of RPS3 remain unclear. Here, we report for the first time that RPS3 is necessary for MM survival and drug resistance. RPS3 was highly expressed in MM, and knockout of RPS3 in MM inhibited cell growth and induced cell apoptosis both *in vitro* and *in vivo*. Overexpression of RPS3 mediated the proteasome inhibitor resistance of MM and shortened the survival of MM tumor-bearing animals. Moreover, our present study found an interaction between RPS3 and the thyroid hormone receptor interactor 13 (TRIP13), an oncogene related to MM tumorigenesis and drug resistance. We demonstrated that the phosphorylation of RPS3 was mediated by TRIP13 via PKCδ, which played an important role in activating the canonical NF-κB signaling and inducing cell survival and drug resistance in MM. Notably, the inhibition of NF-κB signaling by the small-molecule inhibitor targeting TRIP13, DCZ0415, was capable of triggering synergistic cytotoxicity when combined with bortezomib in drug-resistant MM. This study identifies RPS3 as a novel biomarker and therapeutic target in MM.

Introduction

Multiple myeloma (MM), a terminal differentiation of plasma cell hematological malignancy, typically evolves from asymptomatic precursor stages, i.e., monoclonal gammopathy of undetermined significance (MGUS) and smouldering multiple myeloma (SMM), which progress to symptomatic MM.[1,2] MM is characterized by the infiltration of clonal plasma cells into the bone marrow (BM), producing high levels of M-protein (monoclonal globulin or immunoglobulin [Ig] fragment) and inducing end-organ damage, i.e., CRAB – hypercalcemia, renal injury, anemia, and/or bone lesions.[1,2] While the overall survival (OS) of patients with MM has markedly improved with the introduction of chimeric antigen receptor T-cell immunotherapy, autologous stem cell transplantation, and novel agents like proteasome inhibitor bortezomib, immunomodulatory agents, and antibodies targeting cell surface molecules, a large majority of patients still relapse and eventually become refractory owing to the complex genetic heterogeneity and clonal evolution of MM.[3,4] Genomic alterations, including IgH translocations and hyperdiploidy, occur as early as in the precancerous stages MGUS and SMM, from which MM develops.[5] The evolution of MM is reflected in the progressive increase in the number and complexity of genomic alterations, leading to universal aneuploidy and recurrent chromosomal aberrations, which are usually classified as chromosomal instability.[5,6]

Ribosomal protein S3 (RPS3), a component of the 40S subunit of the eukaryotic ribosome, directly participates in ribosome maturation and translation initiation.[7] However, RPS3 is a multifunctional protein implicated in several extra-ribosomal events including DNA repair, apoptosis, selective gene transcription, and host-pathogen interactions, which are mediated by specific post-translational modifications, such as phosphorylation, methylation, and neddylation.[8-11] Notably, RPS3 has been identified as a non-

Rel subunit of nuclear factor-κ B (NF-κB), capable of cooperating with NF-κB Rel proteins to regulate specific NF-κB target gene transcription.[11,12] In resting cells, RPS3 interacts with NF-κB p65-p50-IκBα complexes in the cytoplasm.[11,12] Extracellular stimuli, like tumor necrosis factor α (TNF-α) or lipopolysaccharides, trigger the canonical NF-κB pathway; IκB proteins are phosphorylated by activated IκB kinase (IKK) complex, which then induces the proteasomal degradation of IκB and its degradation from NF-κB complexes; NF-κB Rel complexes and non-Rel subunit RPS3 translocate from the cytoplasm to the nucleus, dramatically stabilizing the binding of NF-κB Rel subunits to specific κB sites that are involved in regulating multiple physiological conditions, e.g., cell survival, apoptosis, radioresistance, and immunoglobulin κ light chain gene expression in B cells.[12-14] However, the detailed biological roles of RPS3 remain largely unknown. The thyroid hormone receptor interactor 13 (*TRIP13*) gene, located on the short arm p15 of chromosome 5, is one of the ten chromosomal instability genes highly linked to MM drug resistance and rapid relapse.[15-17] We previously identified *TRIP13* as an oncogene of MM and demonstrated that overexpression of *TRIP13* promotes MM tumorigenesis, tumor progression, and drug resistance, making it a potentially novel therapeutic target of MM.[15-17] Besides MM, elevated *TRIP13* expression triggers malignant transformation and cancer development in breast cancer, colorectal cancer, lung adenocarcinoma and head and neck cancer.[18-21] The AAA-ATPase TRIP13 protein, a member of a large AAA⁺ protein superfamily of ring-shaped P-loop NTPases, contributes to the regulation of spindle assembly checkpoints and DNA repair pathways during cell division.[22-24] Recently, we have elucidated the crystal structure of wild-type human TRIP13 protein at a resolution of 2.6 Å, based on which we identified the first small-molecule inhibitor of TRIP13, DCZ0415, capable of binding to TRIP13 and exerting potent anti-myeloma activity by impairing DNA repair and inhibiting NF-κB pathway.[17] However, the precise mechanisms of TRIP13 in mediating the drug resistance of MM remains unclear.

Here, we demonstrated for the first time that RPS3 was necessary for MM survival and drug resistance, suggesting that it is a novel potential biomarker and therapeutic target in MM. Moreover, TRIP13-mediated phosphorylation of NF-κB non-Rel subunit RPS3 by PKCδ is important in activating the canonical NF-κB signaling and inducing drug resistance in MM. Notably, the inhibition of NF-κB signaling by DCZ0415 was capable of triggering synergistic drug-resistant MM cytotoxicity when combined with bortezomib.

Methods

Cells and patient samples
Cell lines were purchased from the American Type Culture Collection (Mananssas, VA, USA) or obtained as described in our previous articles.[25,26] All samples were obtained from patients with MM and normal donors who gave informed consent in accordance with the Declaration of Helsinki. Approval was obtained by the Shanghai Tenth People's Hospital Institutional Review Board. Details are available in the *Online Supplementary Appendix*.

Reagents and antibodies
DCZ0415 was synthesized at Shanghai Institute of Materia Medica, Chinese Academy of Sciences. Reagents and antibodies were purchased as detailed in the *Online Supplementary Appendix*.

Plasmids and viral transduction
The full-length cDNA of human TRIP13 and RPS3 were synthesized and cloned into the pLVX-EGFP-IRESpuro (Invitrogen, Carlsbad, CA, USA). The RPS3 mutation was generated by quick change point mutagenesis (Toyobo, Osaka, Japan). Details are available in the *Online Supplementary Appendix*.

In vitro assays
In vitro assays including cell viability, EdU cell proliferation assay, colony formation, apoptosis measurement, cell cycle analysis, quantitative real-time polymerase chain reaction (qRT-PCR), nuclear and cytoplasmic protein extraction, dual-luciferase reporter assay immunoblotting, co-immunoprecipitation (Co-IP) and immunofluorescence were performed as described previously.[17,27] Details are available in the *Online Supplementary Appendix* and *Online Supplementary Table S1*.

CRISPR/Cas9-mediated gene knockout
Knockout cells were generated using lentivirus-mediated CRISPR/Cas9 technology as described previously.[17] The single guided RNA (sgRNA) sequences targeting human TRIP13 was: #1, TGAGTAGCTTTCTAACACTC, #2, CCAAGCTGTCCCAAAGCCCA. The sgRNA sequences targeting human RPS3 were: #1, CTCACCTCTACACTGCCCTC, #2, CTTTCCAGAGGGCAGTGTAG. Details are available in the *Online Supplementary Appendix*.

RNA sequencing
Total RNA was extracted using the RNA-Quick purification kit (ES Science, Shanghai, China) and preserved using TRIZOL (Ambion, Austin, TX, USA), which was sent to OE biotech Co., Ltd. (Shanghai, China) for RNA-sequencing (RNA-seq) analysis. Details are available in the *Online Supplementary Appendix*.

Gene expression analysis using publicly available data sets
The Kaplan-Meier analysis of OS and progression-free survival (PFS) in 436 newly diagnosed MM patients related to RPS3 expression was performed using the database with GSE136324. Gene expression profiles for healthy donors, patients with MM, MGUS, SMM and relapsed MM were performed using the Gene Expression Omnibus data sets (GSE5900 and GSE6477), 208692_at is the probe for RPS3.

Gene expression analysis was performed using Partek Genomic Suite 6.6 with fold changes calculated as relative changes compared to normal plasma cells. Fold changes of at least 2-fold with a $P<0.05$ and a false discovery rate (FDR)<0.05 were considered for further analysis.

Animal studies

MM cells were injected subcutaneously into athymic nude mice (5-week-old). All animal procedures were approved by the Institutional Review Board of the Shanghai Tenth People's Hospital (approval no. SHDSYY-2020-991). Details are available in the *Online Supplementary Appendix*.

Statistical analysis

All data are presented as the mean ± standard deviation of three separate experiments. Statistical significance was determined by Student's *t* test or ANOVA using SPSS v22.0 (IBM, Armonk, NY, USA). $P<0.05$ was considered statistically significant. The CalcuSyn software program (Biosoft, Ferguson, MO, USA) was used to quantify the synergy of the two drugs, and a 95% confidence interval (CI) <1 indicated synergistic activity.

Results

TRIP13 activates the canonical NF-κB signaling

We first determined the role of TRIP13 in regulating NF-κB signaling by using RNA-seq analysis in *TRIP13* overexpressing (TRIP13-OE) and the corresponding empty vector (EV)-transfected ARP-1 cells. The RNA-seq data analysis showed a subset of genes that were differentially expressed upon *TRIP13* overexpression, including 533 upregulated genes and 232 downregulated genes (Figure 1A). The gene set enrichment (GSEA) analysis indicated that overexpression of *TRIP13* in MM cells was positively correlated with NF-κB signaling activation (Figure 1B). In order to confirm the results, we performed immunoblotting to investigate the expression levels of proteins involved in NF-κB signaling and found that TRIP13 overexpression in MM cells effectively elevated levels of p-IKKβ and p-IκBα (Figure 1C). Meanwhile, TNF-α elevated levels of NF-κB downstream p-IκBα, but knockout of TRIP13 in MM cells partly eliminated TNF-α-induced elevation of p-IκBα (Figure 1D). Moreover, we extracted NF-κB p65 proteins in both nucleus and cytoplasm in TRIP13 OE and corresponding EV MM cells and observed that high expression of TRIP13 promoted the translocation of NF-κB p65 into the nuclei (Figure 1E). Similarly, knockout of TRIP13 partly eliminated TNF-α-induced nuclear translocation of NF-κB p65 (Figure 1F).

TRIP13 interacts with NF-κB non-Rel subunit RPS3

We subsequently performed liquid chromatography-tandem mass spectrometry (LC-MS/MS) to identify the potential interacting proteins of TRIP13. TRIP13-tagged Flag (Flag-TRIP13)

and Flag-vector were transfected into HEK293T cells to construct transient strains; TRIP13 and its binding proteins were then purified by Flag beads, and proteins interacting with TRIP13 were identified by mass spectrometry. More than 600 proteins interacting with TRIP13 were identified. We were interested in RPS3 as its key role in regulating NF-κB signaling (Figure 2A). We performed exogenous Co-IP in HEK293T cells transfected with Flag-TRIP13, HA-tagged RPS3 (HA-RPS3), or both constructs and observed that RPS3 interacted with TRIP13 (Figure 2B). We also confirmed the interaction between RPS3 and TRIP13 in ARP-1 cells via endogenous Co-IP (Figure 2C). Immunofluorescence showed that RPS3 was co-localized with TRIP13 in the cytoplasm under normal conditions, which then translocated into the nucleus when NF-κB signaling was activated by TNF-α (Figure 2D).

TRIP13 regulates the phosphorylation of RPS3 via PKCδ

In order to understand the regulatory mechanism of RPS3 and TRIP13, we assessed the PRS3 expression in MM cells (ARP-1 and OCI-MY5) with stable overexpression of TRIP13. There was no significant difference in total RPS3 expression between TRIP13-overexpressed MM cells and the corresponding control (*Online Supplementary Figure S1A*). Meanwhile, knockout of TRIP13 in MM cells using CRISPR-Cas9 had no significant effect on total RPS3 expression (*Online Supplementary Figure S1B*). The phosphorylation status of RPS3 has been studied in conjunction with its biological function. We, therefore, investigated the phosphorylation status of RPS3 in MM cells with stable overexpression of TRIP13 in the presence or absence of TNF-α. RPS3 was immunoprecipitated from TRIP13-OE and the corresponding EV MM cells, and then the phosphorylated residues were enriched by phosphorylated threonine (p-Thr), serine, and tyrosine. We observed that RPS3 was highly phosphorylated at threonine residue(s), especially in the presence of TNF-α (Figure 3A). In order to investigate the mechanism of phosphorylation, we performed mass spectrometry phosphoproteomic analysis to identify the potential phosphorylation sites of RPS3. Interestingly, phosphorylated threonine 221 (T221) on RPS3 was identified as a specific site that was affected by TRIP13 (Figure 3B; *Online Supplementary Figure S2A*). We then mutated the threonine 221 on RPS3 to alanine (T211A) by *in vitro* site-directed mutagenesis to inactivate the original phosphorylation site in MM cells and observed the expression of downstream effector protein p-IκBα in NF-κB signaling. Our results showed that the RPS3 T211A blocked TRIP13-induced phosphorylation of IκBα (Figure 3C), suggesting that the phosphorylation of RPS3 at T221 site is responsible for the TRIP13-driven NF-κB activation. Moreover, we have successfully generated a rabbit polyclonal antibody specific for RPS3 phosphorylated on T221. Immunoblotting analysis revealed a significant upregulation of phosphorylated RPS3 levels upon overexpression of TRIP13 in MM cells (Figure 3D). Subsequently, we conducted an investigation
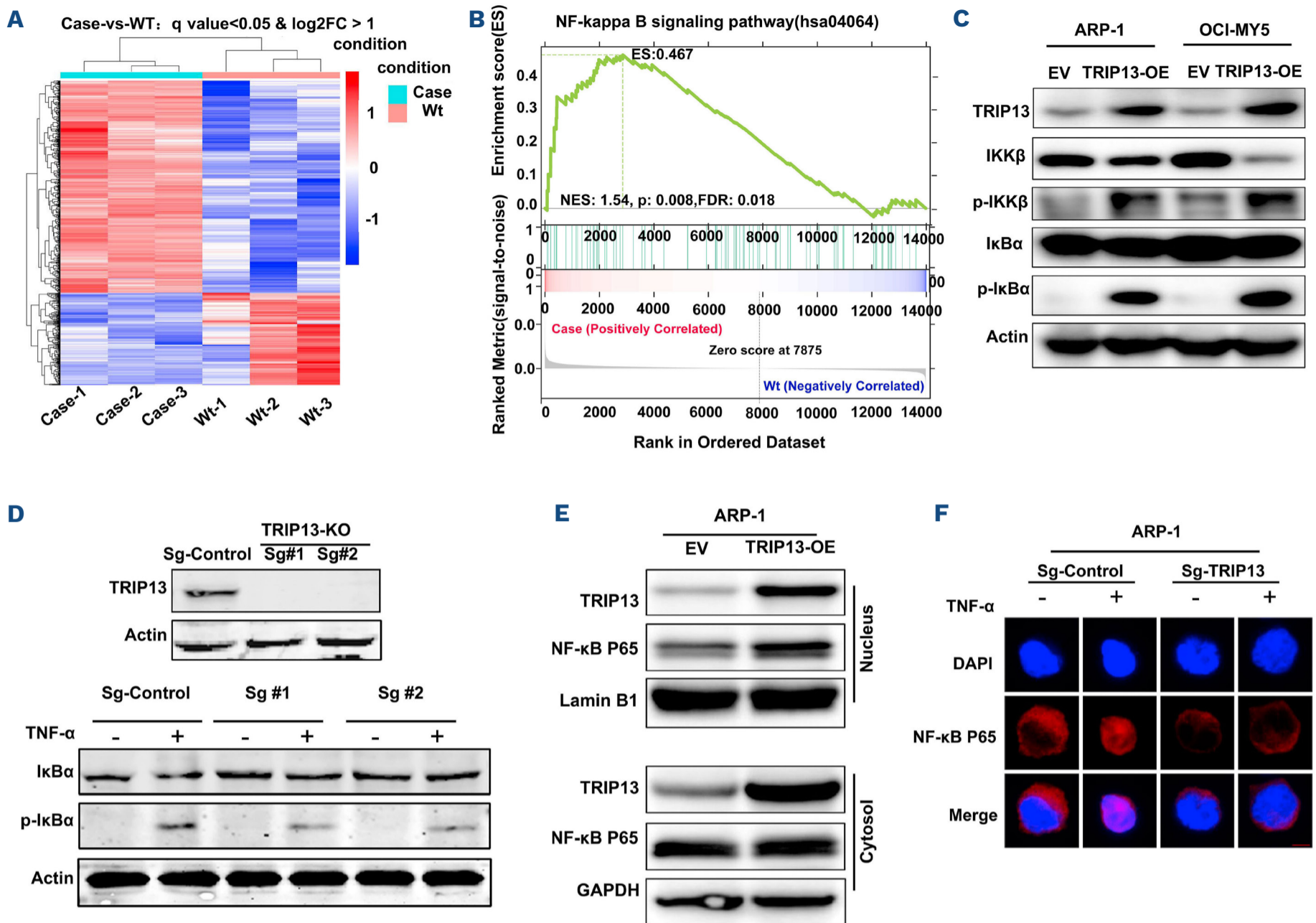
Figure 1. TRIP13 activates the canonical NF-κB signaling. (A) RNA-sequencing analysis of the differentially expressed transcripts in empty vector (EV) and TRIP13-OE ARP-1 cells (red and blue represent high and low mRNA expression levels, respectively). Case represents ARP-1 cells stably transfected with TRIP13-OE; wild-type (wt) represents ARP-1 cells stably transfected with EV. (B) Gene set enrichment analysis (GSEA) indicated a positive correlation between TRIP13 overexpression and NF-κB signallng activation. NES: normalized enrichment score. (C) Immunoblotting analysis of proteins levels involved in canonical NF-κB signaling (IKKβ, p-IKKβ, IκBα, p-IκBα) in EV and TRIP13 OE ARP-1/OCI-MY5 cells. Actin served as a loading control. (D) Immunoblotting confirmed the knockout of TRIP13 (TRIP13-KO) in ARP-1 cells via CRISPR-Cas9 (upper panel). TRIP13-KO or the corresponding control ARP-1 cells were stimulated with or without TNF-α (30 ng/mL, 30 minutes), followed by immunoblotting analysis of IκBα and p-IκBα proteins levels (lower panel). Actin served as a loading control. (E) EV and TRIP13-OE ARP-1 cells were collected. Cytosolic and nuclear proteins were then extracted using a nuclear and cytoplasmic protein extraction kit, followed by immunoblotting analysis of NF-κB p65 levels in the cytoplasm and nucleus. Lamin B1 and GAPDH were used as loading controls for the nucleus and cytoplasm, respectively. (F) Confocal micrographs of TRIP13-KO and the corresponding control ARP-1 cells stimulated with or without TNF-α (30 ng/mL, 30 minutes). The fixed cells were stained with anti-NF-κB p65 (red) and the nuclear dye DAPI (blue). Scale bars =10 μM.

to ascertain the contribution of RPS3 in TRIP13-mediated drug resistance in MM cells. We reduced RPS3 expression in TRIP13-OE MM cells with short interfering RNA targeting RPS3 (siRPS3). Then, the TRIP13-OE, TRIP13-OE+siRPS3, or the EV-transfected MM cells were treated with bortezomib. Consistent with the previous findings, we found that overexpression of TRIP13 induced bortezomib resistance in MM; knockdown of RPS3 re-sensitized the effects of bortezomib on TRIP13-OE MM cells (Figure 3E).

Protein kinase C δ (PKCδ) is a serine-threonine protein kinase that has been demonstrated to phosphorylate T221 residues of RPS3.[28,29] In order to further validate the involvement of phosphorylation of T221 in the TRIP13-driven canonical NF-κB activation, we first performed endogenous Co-IP with TRIP13 antibody in ARP-1 cells and observed an interaction of RPS3, TRIP13, and PKCδ (Figure 3F). Then, TRIP13-OE or EV MM cells (ARP-1/OCI-MY5) were treated with a potent and selective PKCδ inhibitor, BJE6-106. Immunoblotting showed that BJE6-106 suppressed TRIP13-induced activation of proteins in NF-κB signaling (Figure 3G), suggesting that PKCδ is responsible for the TRIP13-driven canonical NF-κB activation. We also determined the effect of BJE6-106 on
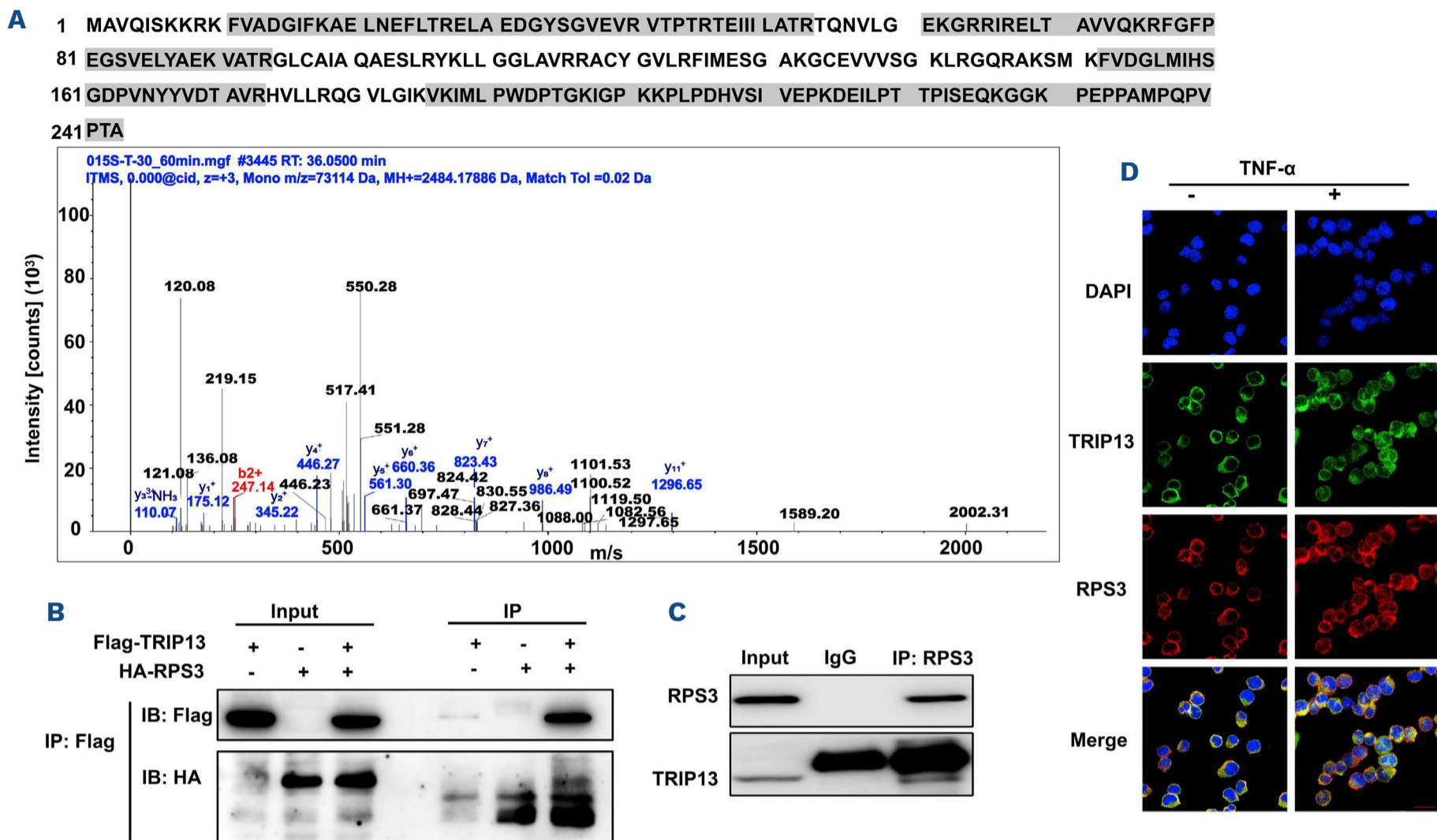
Figure 2. TRIP13 interacts with NF-κB non-Rel subunit RPS3. (A) Peptides (upper panel, shaded regions) of RPS3, identified via mass spectrometry. Characteristic peptides of RPS3 identified by secondary mass spectrogram (lower panel). (B) HEK293T cells were transfected with Flag-TRIP13, HA-RPS3, or both constructs. Cell lysates were immunoprecipitated using anti-Flag and the immunoprecipitants or input were analyzed by immunoblotting with anti-HA or anti-Flag. (C) Endogenous co-immunoprecipitation was conducted with ARP-1 cells using anti-RPS3, followed by immunoblotting using anti-TRIP13 or anti-RPS3. Anti-IgG was used as a non-specific control. (D) Confocal micrographs of ARP-1 cells stimulated with or without TNF-α (30 ng/mL, 30 minutes). The fixed cells were stained with anti-TRIP13 (green), anti-RPS3 (red), and the nuclear dye DAPI (blue). Scale bars =10 μM.

the transcriptional activity of NF-κB in TRIP13-OE or EV MM cells by using a dual-luciferase reporter assay. The results revealed that overexpression of TRIP13 induced significant activation of NF-κB transcription, but the effect could be reversed by BJE6-106 (Figure 3H). We previously demonstrated that overexpression of TRIP13 induced bortezomib resistance in MM cells.[15,17] We further determined whether PKCδ inhibitor could overcome TRIP13-induced bortezomib resistance of MM cells. TRIP13-OE or EV MM cells were treated with BJE6-106 in the presence or absence of bortezomib. Consistently, we observed that bortezomib significantly suppressed cell viability of EV MM cells but had no obvious effect on TRIP13-OE MM cells (*Online Supplementary Figure S2B*). Additionally, a significant decrease of cell viability was observed in TRIP13-OE MM cells in the presence of BJE6-106 and bortezomib (*Online Supplementary Figure S2B*).

RPS3 is highly expressed in multiple myeloma and is required for multiple myeloma survival *in vitro* and *in vivo*
We determined the expression of RPS3 in MGUS, SMM, MM, relapsed MM and normal donors in two independent publicly available data sets. RPS3 was significantly overex-

pressed in MGUS, SMM, MM and relapsed MM compared to that in the corresponding normal donors (Figure 4A). We also compared the *RPS3* messenger RNA (mRNA) levels in CD138-enriched plasma cells from five patients with MM and peripheral blood mononuclear cells from normal donors using qRT-PCR and confirmed high levels of *RPS3* mRNA in MM (*Online Supplementary Figure S3A*). We further examined RPS3 expression using immunoblotting and observed upregulated RPS3 protein levels in patients with MM compared to that in the normal donors (Figure 2B). Meanwhile, immunohistochemistry using BM biopsies from patients with MM and normal donors showed higher RPS3 expression in MM than in the normal donors (*Online Supplementary Figure S3B*). Additionally, the Kaplan-Meier analysis showed that MM patients with higher RPS3 expression had significantly shorter overall survival and PFS (Figure 4C).

In order to elucidate the biological function of RPS3, RPS3 expression in MM cells (ARP-1/OCI-MY5) was stably knocked out using sgRNA targeting *RPS3* (sg-RPS3) by CRISPR-Cas9 (Figure 4D). Results from Cell Counting Kit (CCK)-8 and EdU cell proliferation assays showed that knockout of RPS3 significantly suppressed proliferation of MM cells (Figure 4E;

Online Supplementary Figure S3C). Cell apoptosis analysis showed that RPS3 knockout induced significant MM cell apoptosis (*Online Supplementary Figure S3D*), which was further supported by increased levels of cleaved caspase

3/8/9 proteins in sg-RPS3 MM cells (*Online Supplementary Figure S3E*). Additionally, cell-cycle analysis suggested that knockout of RPS3 disrupted cell-cycle progression, with G2/M-phase arrest (*Online Supplementary Figure S3F*). Con-
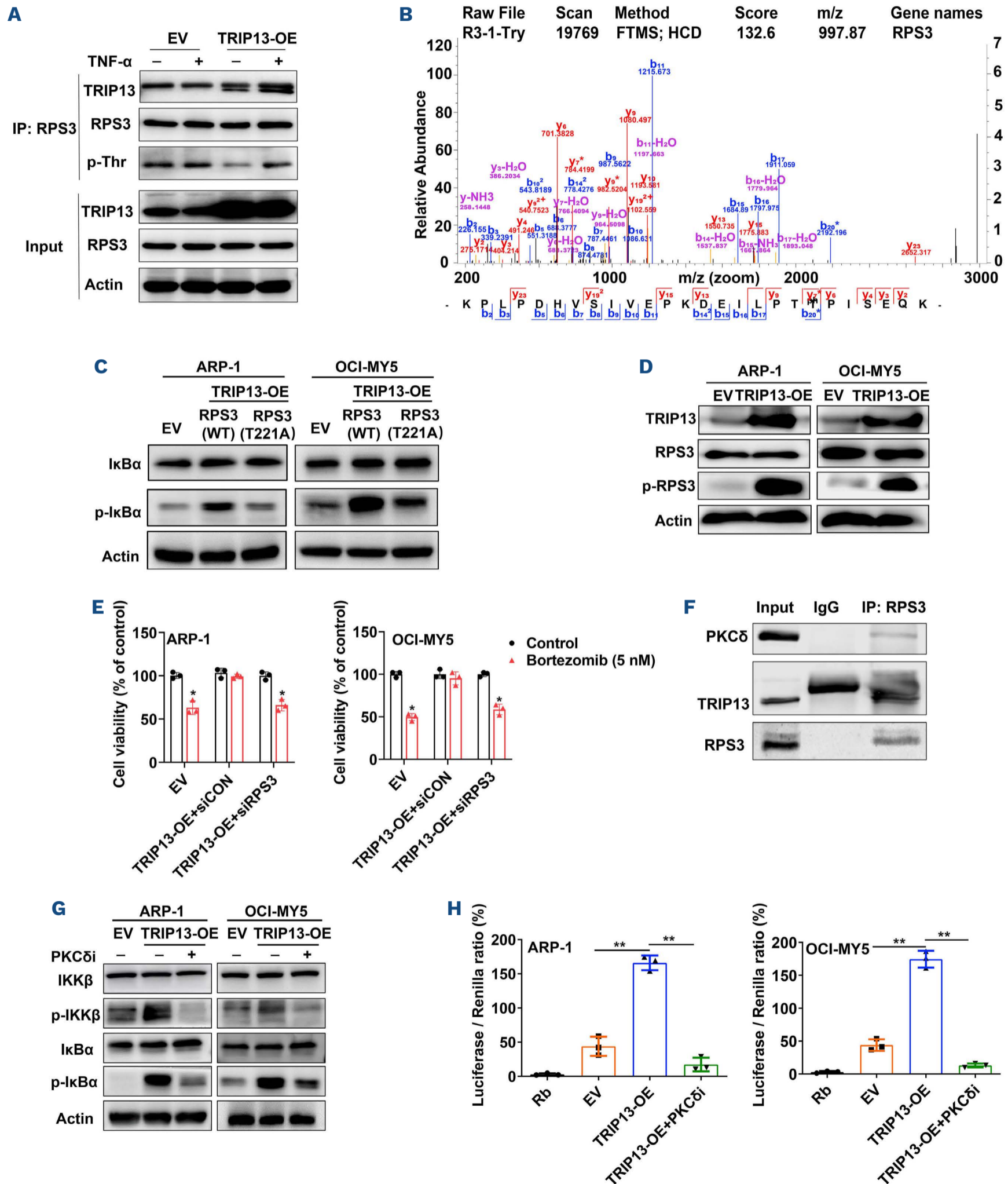
Continued on following page.

Figure 3. TRIP13 regulates the phosphorylation of RPS3 via PKCδ. (A) ARP-1 cells stably transfected with lentivirus-mediated human TRIP13-cDNA (TRIP13-OE) or the empty vector (EV) were stimulated with or without TNF-α (30 ng/mL, 30 minutes). Cell lysates were immunoprecipitated using anti-RPS3 and the immunoprecipitants or input were analyzed by immunoblotting with anti-TRIP13, anti-RPS3, anti-phosphorylated threonine (p-Thr). Actin served as a loading control. (B) Mass spectrometry phosphoproteomic analysis identified phosphorylated threonine 221 (T221) on RPS3. (C) Threonine 221 on RPS3 was mutated to alanine (T211A). EV and TRIP13-OE multiple myeloma (MM) cells were then transfected with RPS3 (WT) or T211A, followed by immunoblotting with IκBα or p-IκBα antibodies. Actin served as a loading control. (D) Immunoblotting detection of protein levels of *RPS3* and phosphorylated RPS3 (p-RPS3) in EV and TRIP13-OE ARP-1/OCI-MY5 cells. Actin served as a loading control. (E) TRIP13-OE transfected with short interfering RNA targeting RPS3 (TRIP13-OE+siRPS3) or siCON (TRIP13-OE+siCON), or EV ARP-1 (left panel) and OCI-MY5 (right panel) MM cells were treated with vehicle or bortezomib (5 nM) for 48 hours, followed by CCK-8 assay analysis of cell viability. Data are shown as mean ± standard deviation with *P* value based on unpaired *t* test (N=3, *P<0.05, **P<0.01). The experiments were repeated 3 times. (F) Endogenous co-immunoprecipitation was conducted with ARP-1 cells using anti-TRIP13, followed by immunoblotting using anti-TRIP13, anti-PKCδ, or anti-RPS3. Anti-IgG was used as a non-specific control. (G) EV and TRIP13-OE MM cells were treated with the 0.1 μM PKCδ inhibitor (PKCδi), BJE6-106, for 24 hours, followed by immunoblotting with IKKβ, p-IKKβ, IκBα or p-IκBα antibodies. Actin served as a loading control. (H) EV and TRIP13-OE ARP-1 (left panel) and OCI-MY5 (right panel) MM cells were transiently transfected with NF-κB luciferase reporter. The cells were then treated with or without 0.1 μM PKCδi (BJE6-106) for 24 hours, followed by a dual-luciferase reporter assay analysis of NF-κB transcriptional activity. Data are shown as mean ± standard deviation with *P* value based on unpaired *t* test (N=3, **P<0.01). The experiments were repeated 3 times.

sistently, immunoblotting demonstrated that RPS3 knockout significantly reduced the levels of G2/M-phase-related proteins including CDC25C, Cyclin B1, and CDK1 (*Online Supplementary Figure S3G*). In order to further evaluate the efficacy of RPS3 in MM growth *in vivo*, we established a MM xenograft model via subcutaneous injection of RPS3-knockout ARP-1 or the corresponding control cells in nude mice. As expected, RPS3 knockout significantly suppressed tumor growth *in vivo* (Figure 4F; *Online Supplementary Figure S3H*). Meanwhile, much lower tumor weight was observed in the RPS3-knockout group than in the control group (*Online Supplementary Figure S3I*). Additionally, immunohistochemistry showed that the proliferation marker Ki-67 was obviously decreased in the RPS3 knockout group than in the control (*Online Supplementary Figure S3J*). TUNEL assays revealed that RPS3 knockout induced increased cell apoptosis compared to the control (*Online Supplementary Figure S3J*).

RPS3 overexpression induces proteasome inhibitor resistance in multiple myeloma and is negatively correlated with multiple myeloma survival
We overexpressed RPS3 in the MM cells (ARP-1/OCI-MY5) using lentivirus-mediated human RPS3-cDNA (Figure 5A). We first evaluated the effect of RPS3 on MM proliferation with *RPS3* overexpressed (RPS3-OE) or the empty vector (EV)-transfected MM cells. CCK-8 and EdU cell proliferation assays showed that overexpression of RPS3 significantly increased proliferation of MM cells (Figure 5B; *Online Supplementary Figure S4A*). RPS3-OE or EV-transfected MM cells were then treated with increasing concentrations of proteasome inhibitors bortezomib or carfizomib. Interestingly, we found that the proteasome inhibitors significantly decreased the cell viability of EV MM cells but had no obvious effects on RPS3-OE MM cells (Figure 5C; *Online Supplementary Figure S4B*). Additionally, colony formation assay showed that while RPS3 overexpression increased colony formation of MM, the proteasome inhibitors decreased the colony formation rate of EV MM cells but had a much less

effect on RPS3-OE MM cells (*Online Supplementary Figure S4C, D*). In order to further examine the *in vivo* efficacy of RPS3-induced drug resistance of MM, RPS3-OE or EV ARP-1 cells implanted subcutaneously in nude mice were treated with bortezomib or the vehicle. Consistent with the findings *in vitro*, we observed that bortezomib significantly suppressed tumor growth in the EV group but had no obvious effect on tumors in the RPS3-OE nude mice (Figure 5D; *Online Supplementary Figure S4E*). Meanwhile, immunohistochemistry showed an increase in Ki-67 expression in RPS3-OE tumors (*Online Supplementary Figure S4F*). Additionally, RPS3-OE mice treated with or without bortezomib displayed a significant decrease in survival as compared to that in mice in the EV or EV + bortezomib group (Figure 5E).

DCZ0415 synergizes with bortezomib in drug-resistant multiple myeloma cells *in vitro* and *in vivo*
Proteins involved in NF-κB signaling were activated in bortezomib-resistant (BR) cells (*Online Supplementary Figure S5A*). We also evaluated the expression of RPS3 at both mRNA and protein levels, including both total and phosphorylated forms, in isogenic pair of MM cell lines with induced resistance to bortezomib (H929/H929R and RPMI-8226/RPMI-8226R5). We observed a notable upregulation of p-RPS3 in BR MM cells, while no significant differences were found in the expression levels of RPS3 at both mRNA (*data not shown*) and total protein levels when comparing BR MM cells with their sensitive counterparts (*Online Supplementary Figure S5A*). Our previous paper demonstrated that DCZ0415, a small inhibitor specifically targeting TRIP13, induced cell death by inhibiting the NF-κB signaling pathway.[17] We further investigated the effects of DCZ0415 on NF-κB signaling. Immunoblotting showed that DCZ0415 significantly inactivated proteins (p-IKKβ, p-p65, and p-IκBα) involved in NF-κB signaling (*Online Supplementary Figure S5B*). Meanwhile, immunofluorescence observed that DCZ0415 effectively hijacked the nuclear translocation of NF-κB p65 in H929R cells (*Online Supplementary Figure S5C*). In order to gain
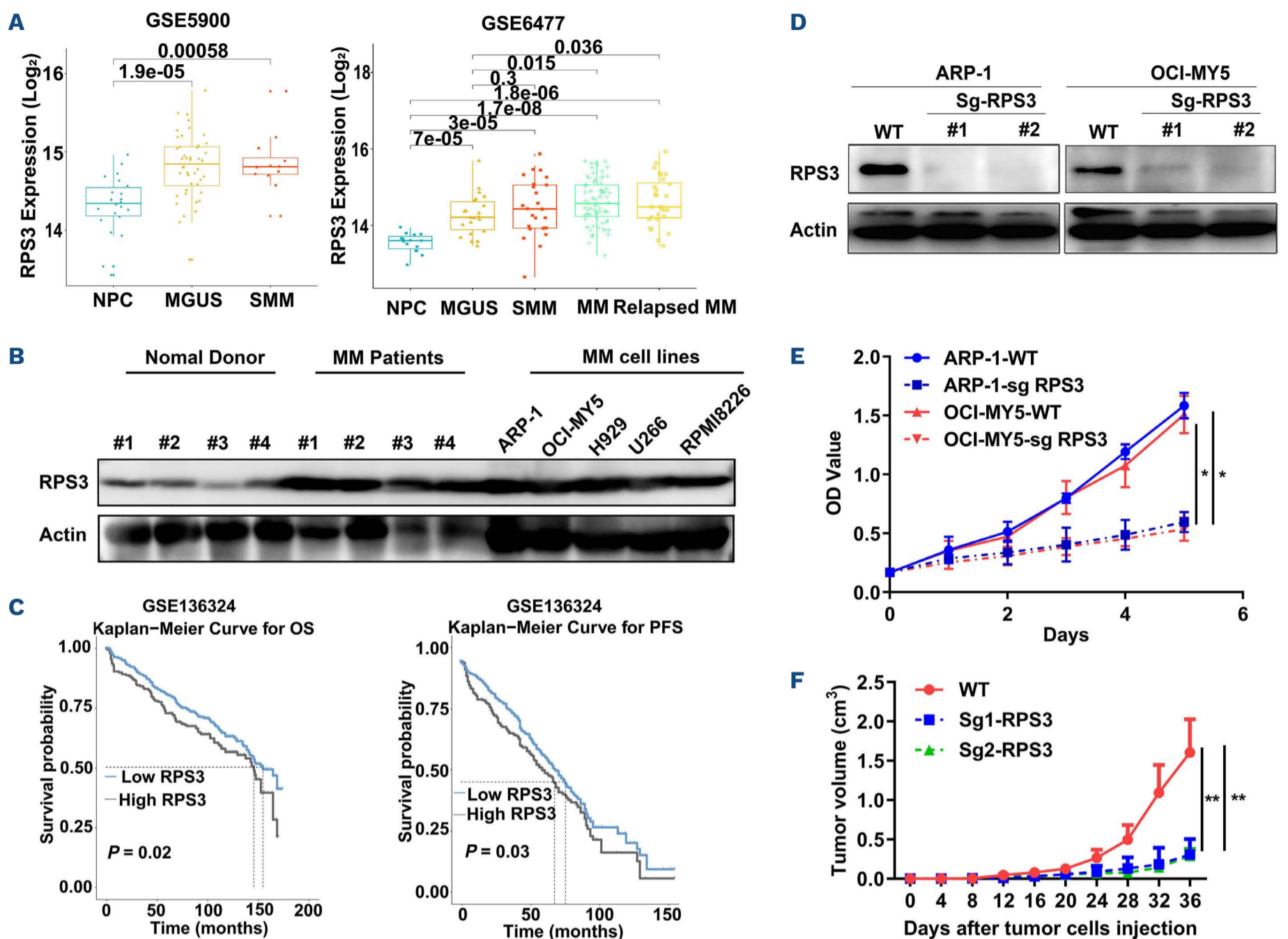
Figure 4. RPS3 is overexpressed in multiple myeloma and is required for multiple myeloma survival *in vitro* and *in vivo*. (A) Analysis of RPS3 expression in normal donors (NPC), monoclonal gammopathy of undetermined significance (MGUS), smouldering multiple myeloma (SMM), multiple myeloma (MM) and relapsed MM by using 2 independent publicly available data sets from NCBI Gene Expression Omnibus (GEO) database under accession numbers (left GSE5900, right GSE6477). Statistics were calculated using Wilcoxon rank sum test. (B) Immunoblotting showed upregulated RPS3 protein levels in patients with MM and MM cell lines compared with that of the normal donors. Actin served as a loading control. (C) Kaplan-Meier curves of overall survival (OS) and progression-free survival (PFS) in 436 newly diagnosed MM patients related to RPS3 expression. The dataset was obtained from NCBI GEO database with GSE136324. Significant differences were calculated by log-rank Mantel-Cox test. (D) Immunoblotting confirmed the knockout of RPS3 in MM cells (ARP-1/OCI-MY5) by single guided RNA (sgRNA) targeting *RPS3* (Sg-RPS3) using CRISPR-Cas9. Sg-Control represents MM transfected with empty vector (EV). Actin served as a loading control. (E) Cell survival of MM transfected with Sg-RPS3 or Sg-Control was measured by CCK-8 assay. The Y-axis represents the optical density (OD) value corresponding to the viability of the cells. Data are shown as mean ± standard deviation with *P* value based on two-way ANOVA (N= 3, *$P<0.05$). The experiments were repeated 3 times. (F) ARP-1 cells transfected with Sg-RPS3 or Sg-Control were subcutaneously injected into nude mice. Graphic represents curves of the tumor growth in nude mice. Data are shown as mean ± standard deviation with *P* value based on two-way ANOVA (N= 5, **$P<0.01$).

further insights into the mechanistic effects of DCZ0415, we conducted additional investigations on its impact on RPS3 expression. MM cells were treated with increasing doses of DCZ0415, or TRIP13-OE MM cells were treated with or without DCZ0415. Immunoblotting revealed a significant reduction in p-RPS3 levels upon treatment with DCZ0415 in both MM cells and TRIP13-OE MM cells, indicating that the TRIP13/RPS3 axis might be involved in DCZ0415-induced cell death (Figure 6A, B). We further determined the effects

of DCZ0415 on *RPS3*-knockout or the sgControl-transfected wild-type MM cells, and observed that knockout of *RPS3* significantly reduced the sensitivity of MM cells to DCZ0415 (Figure 6C). In order to determine whether the effects of DCZ0415 on drug-resistant cells was dependent on TRIP13-RPS3 axis, we treated TRIP13-OE, TRIP13-OE+siRPS3, or the corresponding EV cells with increasing doses of DCZ0415. CCK-8 assay revealed that treatment of TRIP13-OE cells with DCZ0415 exhibited augmented cytotoxicity, while this
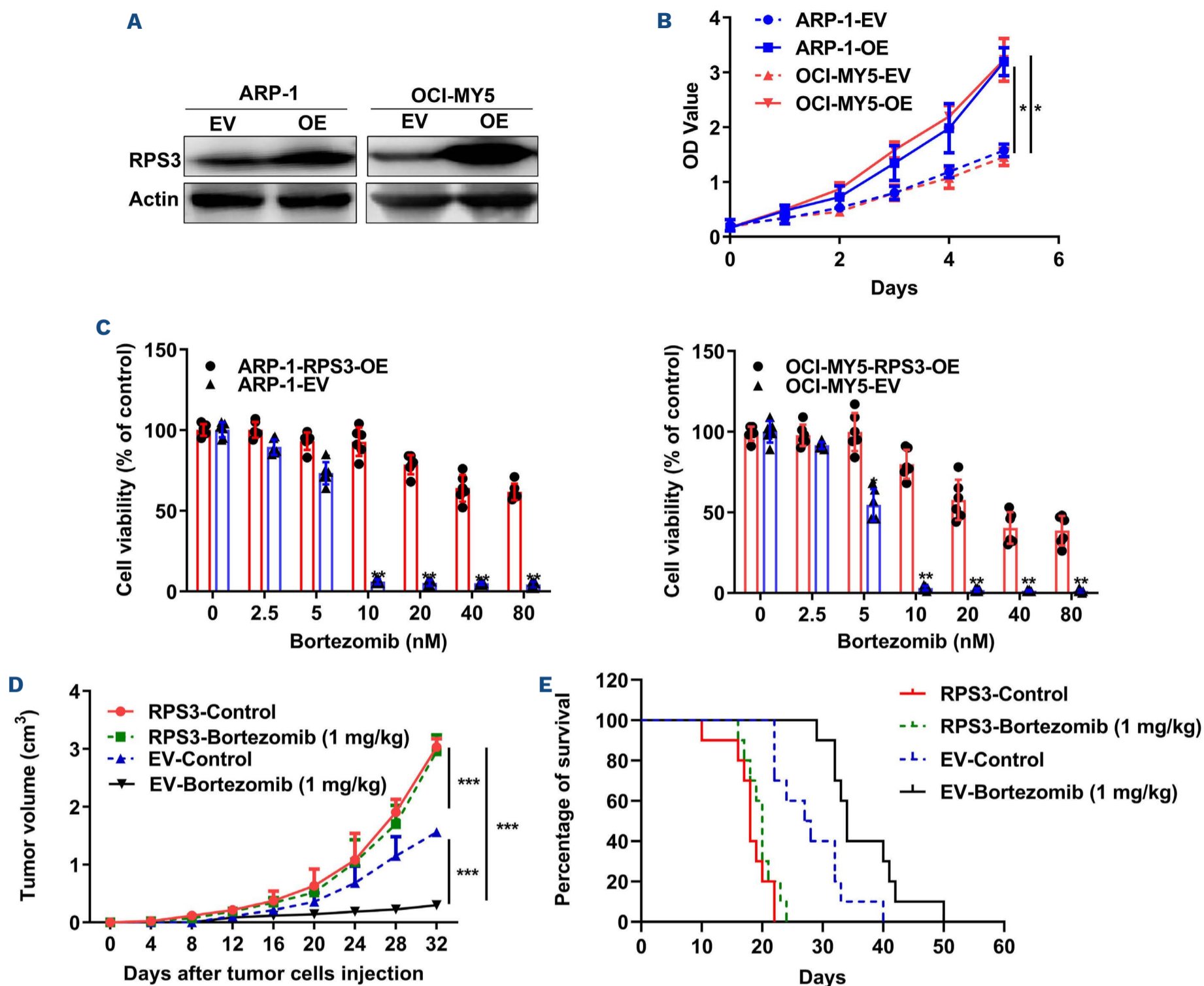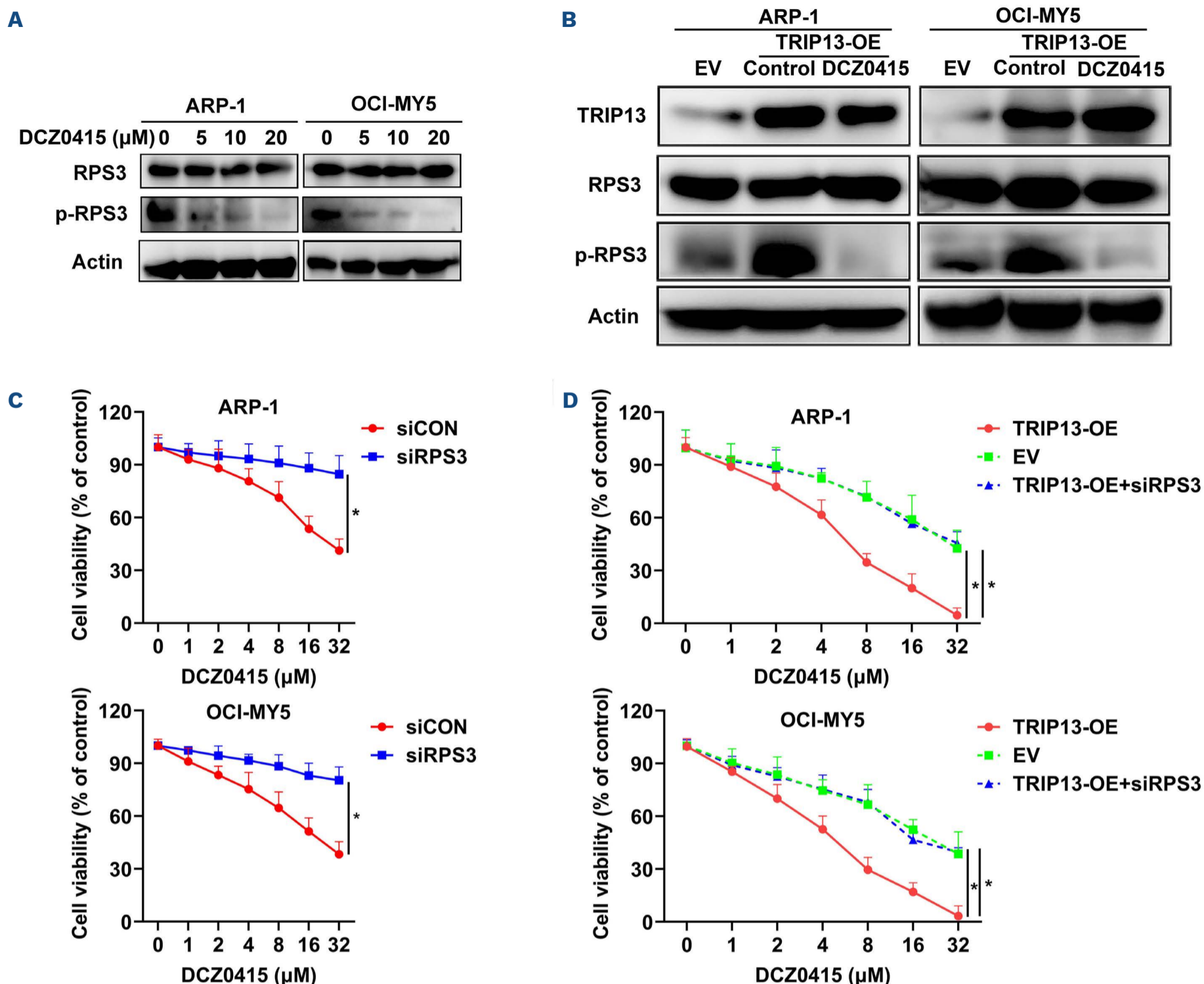
Figure 5. RPS3 overexpression induces proteasome inhibitor resistance in multiple myeloma and is negatively correlated with multiple myeloma survival. (A) Immunoblotting confirmed overexpression of RPS3 in multiple myeloma (MM) cells (ARP-1/OCI-MY5) stably transfected with lentivirus-mediated human *RPS3*-cDNA (RPS3-OE). EV represents MM cells stably transfected with empty vector. Actin served as a loading control. (B) Cell survival of MM transfected with RPS3-OE or EV was measured by CCK-8 assay. The Y-axis represents the optical density (OD) value corresponding to the viability of the cells. Data are shown as mean ± standard deviation (SD) with *P* value based on two-way ANOVA (N= 3, *$P<0.05$). The experiments were repeated 3 times. (C) CCK-8 assay examined cell viability of RPS3-OE or EV MM cells treated with increasing doses of bortezomib (0-80 nM) for 48 hours. Data are shown as mean ± SD with *P* value based on unpaired *t* test (N= 6, **$P<0.01$). The experiments were repeated 3 times. (D) RPS3-OE and EV ARP-1 cells implanted subcutaneously in nude mice were treated with bortezomib (1 mg/kg, twice/week) or vehicle. Graphic represents curves of the tumor growth. Data are shown as mean ± SD with *P* value based on two-way ANOVA (N= 3, ***$P<0.001$). (E) RPS3-OE and EV ARP-1 cells implanted subcutaneously in nude mice were treated with bortezomib (1 mg/kg, twice/week) or vehicle. Kaplan-Meier and log-rank analysis of the median overall survival of mice in the 4 groups. Significant differences were calculated by log-rank Mantel-Cox test (N=10, EV-Control *vs.* EV-Bortezomib, *P*=0.0059; EV-Control *vs.* RPS3-Control, *P*<0.0001; EV-Bortezomib *vs.* OE-Bortezomib, *P*<0.0001; RPS3-Control *vs.* OE Bortezomib, non-significant).

effect was partially attenuated upon knockdown of RPS3 (Figure 6D). These findings indicate that DCZ0415 holds immense potential for drug resistant MM. We further determined the effects of DCZ0415 on drug resistance in MM. BR MM cells (H929R and RPMI-8226R5) were first treated with increasing doses of DCZ0415 for 72 h. CCK-8 assay showed that DCZ0415 significantly decreased cell viability of H929R/RPMI-8226R cells in a dose-dependent manner (*Online Supplementary Figure S6A*). Flow cytometry revealed that DCZ0415 significantly promoted apoptosis of BR cells, which was further supported by increased levels of cleaved caspase-3/8/9 and PARP proteins in BR cells treated with

Figure 6. The antimyeloma activity of DCZ0415 is dependent on TRIP13-RPS3 axis. (A) Multiple myeloma (MM) cells (ARP-1 and OCI-MY5) were treated with increasing doses of DCZ0415 (0-20 μM) for 72 hours (h), followed by immunoblotting detection of RPS3 and p-RPS3 levels. Actin served as a loading control. (B) Empty vecotor (EV) or TRIP13-OE MM cells treated with or without DCZ0415, followed by immunoblotting detection of TRIP13, RPS3 and p-RPS3 levels. Actin served as a loading control. (C) MM cells (ARP-1 and OCI-MY5) transfected with siRPS3 or the corresponding control (siCON) were treated with increasing doses of DCZ0415 (0-32 μM) for 72 h, followed by CCK-8 assay analysis of cell viability. Data are shown as mean ± standard deviation with *P* value based on two-way ANOVA (N= 3, *$P<0.05$). (D) TRIP13-OE+siRPS3, TRIP13-OE+siCON, or the corresponding EV cells with increasing doses of DCZ0415 for 72 h, followed by CCK-8 assay analysis of cell viability. Data are shown as mean ± standard deviation with *P* value based on two-way ANOVA (N= 3, *$P<0.05$).

DCZ0415 (*Online Supplementary Figure S6B, C*). We further determined the effects of DCZ0415 in combination with bortezomib. Colony formation assay showed that bortezomib alone had no obvious effect on colony formation rates of BR cells, but treatment with bortezomib in combination with DCZ0415 had much lower colony formation rates than that of those treated with DCZ0415 or bortezomib alone (*Online Supplementary Figure S6D*), suggesting that DCZ0415 treatment resensitized BR MM cells. Additionally, the median dose effect analysis was used to calculate the CI values

between DCZ0415 and bortezomib. Interestingly, we found a high synergy between DCZ0415 and bortezomib, with the CI values <1 both in H929R and RPMI-8226R5 MM cells (Figure 7A). Additionally, immunoblotting showed that the combination of DCZ0415 and bortezomib induced an observable decrease in levels of p-IKKβ and p-IκBα in both H929R and RPMI-8226R5 cells (Figure 7B). We also determined whether DCZ0415 treatment could enhance the sensitivity of BR MM cells to bortezomib *in vivo* by establishing a MM xenograft model using nude mice subcutaneously injected
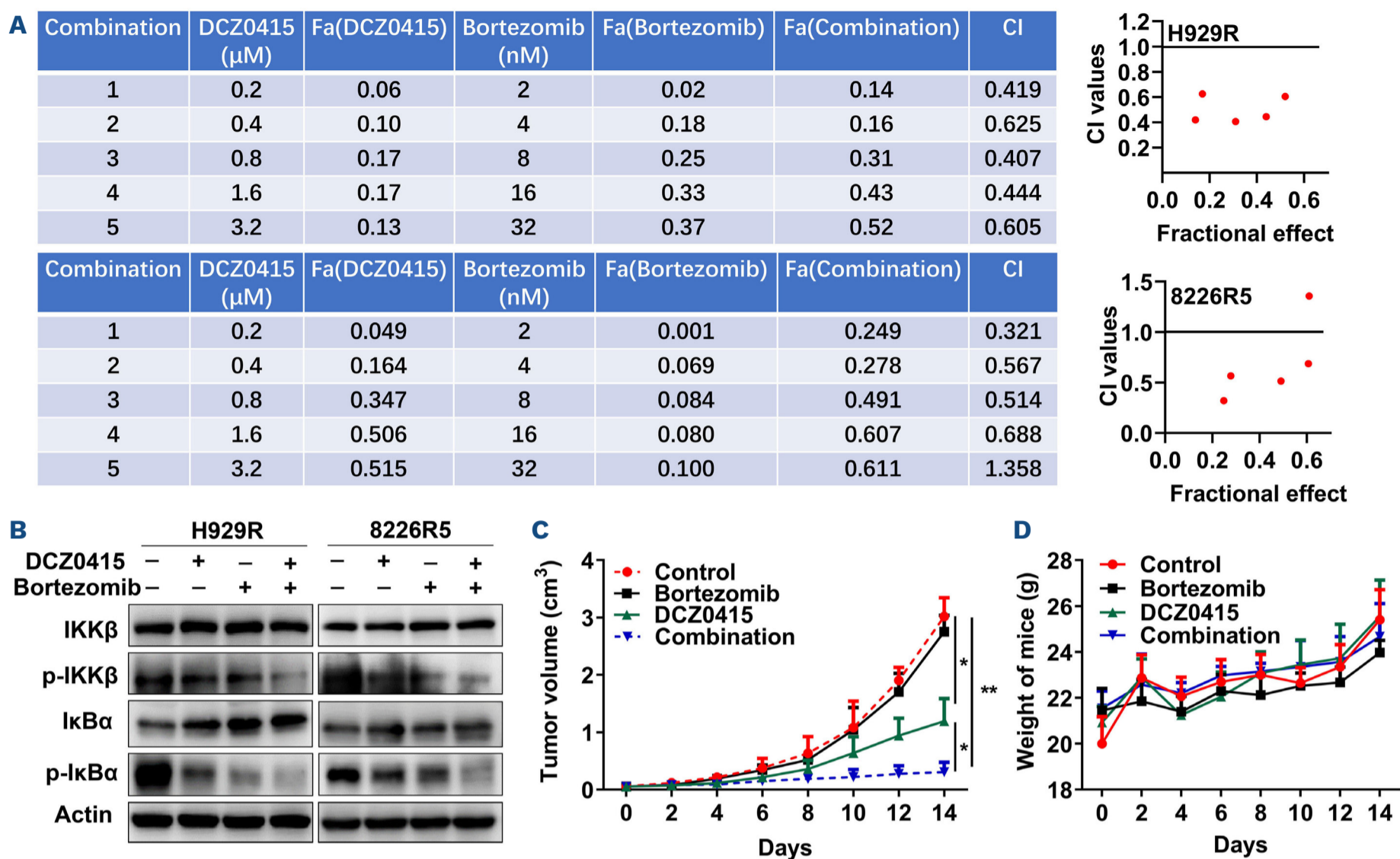
A

Combination	DCZ0415 (µM)	Fa(DCZ0415)	Bortezomib (nM)	Fa(Bortezomib)	Fa(Combination)	CI
1	0.2	0.06	2	0.02	0.14	0.419
2	0.4	0.10	4	0.18	0.16	0.625
3	0.8	0.17	8	0.25	0.31	0.407
4	1.6	0.17	16	0.33	0.43	0.444
5	3.2	0.13	32	0.37	0.52	0.605

Combination	DCZ0415 (µM)	Fa(DCZ0415)	Bortezomib (nM)	Fa(Bortezomib)	Fa(Combination)	CI
1	0.2	0.049	2	0.001	0.249	0.321
2	0.4	0.164	4	0.069	0.278	0.567
3	0.8	0.347	8	0.084	0.491	0.514
4	1.6	0.506	16	0.080	0.607	0.688
5	3.2	0.515	32	0.100	0.611	1.358

B **C** **D**

Figure 7. DCZ0415 synergizes with bortezomib in drug-resistant multiple myeloma cells *in vitro* and *in vivo*. (A) H929R (upper panel) and RPMI-8226R5 (lower panel) cells were treated with vehicle, bortezomib (2-32 nM), and DCZ0415 (0.2-3.2 µM) alone or in combination for 72 hours (h), followed by CCK-8 assay analysis of cell viability. Confidence interval (CI) values were calculated using the Chou–Talalay method (right panel). (B) Immunoblotting detection of the protein levels of IKKβ, p-IKKβ, IκBα, and p-IκBα in H929R (left panel) and RPMI-8226R5 (right panel) cells treated with the medium, bortezomib (20 nM), and DCZ0415 (10 µM) alone or in combination. (C, D) Nude mice bearing H929R multiple myeloma (MM) tumors were treated with vehicle, bortezomib (1 mg/kg, twice/week), and DCZ0415 (50 mg/kg, twice/week) alone or in combination. (C) Graphic represents curves of the tumor growth. Data are shown as mean ± standard deviation with *P* value based on two-way ANOVA (N=4, *P<0.05, **P<0.01). (D) Weight of mice.

with H929R cells. Consistent with the findings *in vitro*, we observed that DCZ0415 treatment was pivotal in re-sensitizing BR MM cells *in vivo* (Figure 7C; *Online Supplementary Figure S6E, F*). Meanwhile, the body weights of the mice had no significant difference among groups during treatment (Figure 7D). Moreover, immunohistochemistry and TUNEL assays showed that the co-administration of DCZ0415 and bortezomib induced a decrease in Ki-67 and an increase in apoptosis, compared with that in the vehicle, DCZ0415, or bortezomib alone (*Online Supplementary Figure S6G*).

Discussion

The development of drug resistance is a clinical challenge observed in a variety of therapeutic approaches. Despite the establishment of novel therapeutic interventions, MM remains invariably incurable owing to the development of drug resistance and subsequent relapse.[30]

RPS3 can interact with the p65 subunit of NF-κB, thereby facilitating NF-κB binding to DNA and preferentially directing it to specific κB sites in the promoters of target genes.[11,12] Other studies have shown that the inhibitor of κB kinase β (IKKβ) can phosphorylate RPS3 at serine 209 and enhance the binding of phosphorylated RPS3 with importin-α, facilitating RPS3 entry into the nuclear transporter pathway.[13] IKKβ is the major kinase that phosphorylates IκBα, leading to its degradation from NF-κB complexes.[12] The NF-κB dimers translocate into the nucleus, where they bind to specific DNA sites and activate the transcription of target genes.[12] It has been reported that the secreted RPS3 protein is an indicator of some malignant tumors.[14,31,32] RPS3 is capable of regulating melanoma cell growth and apoptosis by targeting Cyto C/Ca^{2+}/MICU1-dependent mitochondrial signaling.[32] Moreover, RPS3 is a key control point of radioresistance in glioblastoma and non-small cell lung cancer by promoting the repair of DNA damage.[14,33] Here, we found for the first time that RPS3 was significantly overexpressed in MM, and
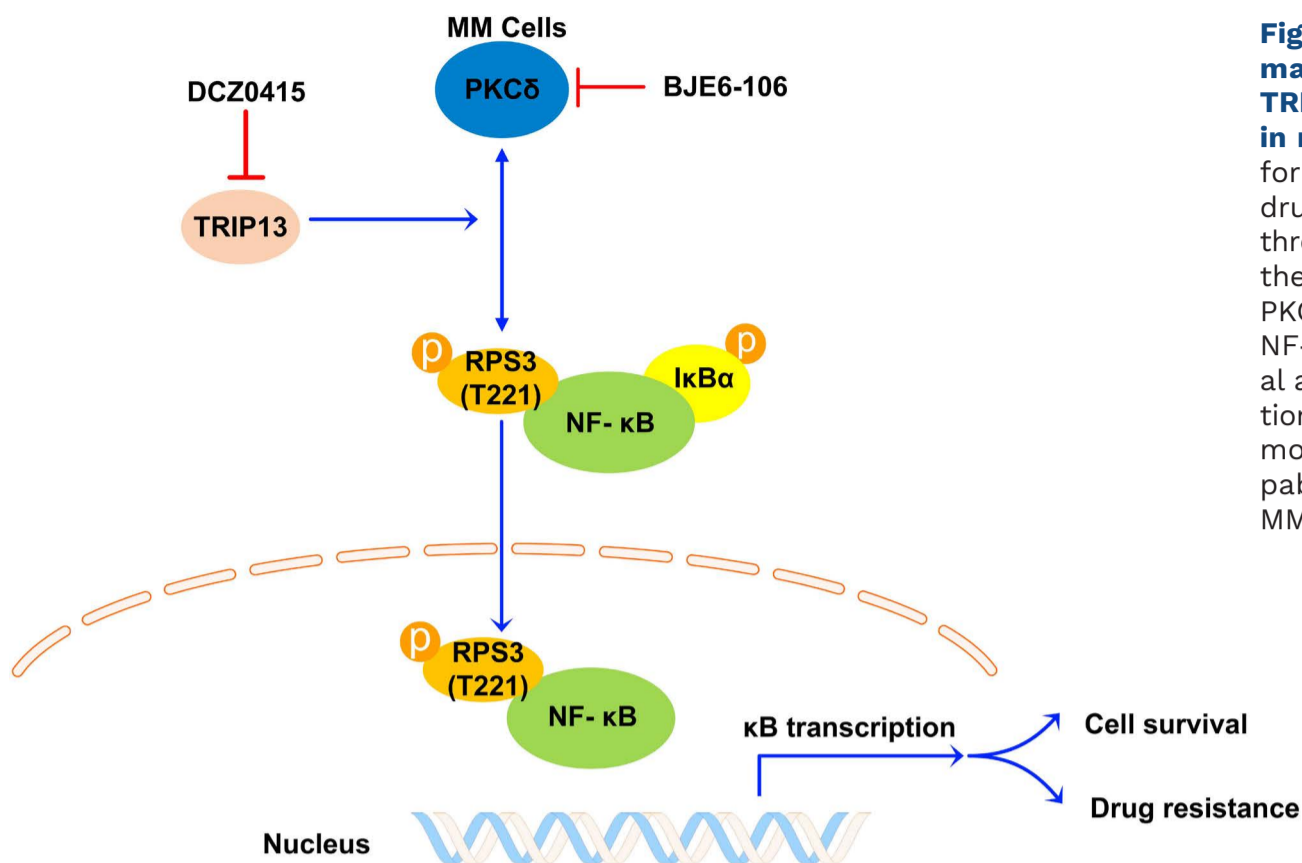
Figure 8. A working model depicting the major molecular mechanisms of the TRIP13-PKCδ/PRS3/ NF-κB signaling axis in multiple myeloma. RPS3 is necessary for multiple myeloma (MM) survival and drug resistance. TRIP13 acts as a mediator through binding PKCδ and RPS3 to promote the phosphorylation activation of RPS3 by PKCδ, which further activates canonical NF-κB signaling and inducing cell survival and drug resistance of MM. The inhibition of NF-κB signaling by DCZ0415, a small molecule inhibitor targeting TRIP13, is capable of overcoming drug resistance of MM cells.

its overexpression status correlated with poor prognosis of patients with MM. The knockout of *RPS3* could induce cell cycle arrest and cell apoptosis in MM. Importantly, overexpression of RPS3 could promote MM proliferation and confer proteasome inhibitor resistance to MM, as demonstrated in a mouse model which showed that RPS3 overexpression could significantly shorten survival even under the treatment of bortezomib. Our findings in the current study first demonstrate that RPS3 is closely associated with drug resistance and poor prognosis in MM. RPS3 could be a potential therapeutic target of MM. The small molecule inhibitors specifically targeting RPS3 could be developed for the treatment of MM and to overcome proteasome inhibitor resistance.

TRIP13 is identified as a driver of B-cell malignancies.[15-17] We previously demonstrated that overexpression of TRIP13 is functionally linked to drug resistance of MM, and inhibition of TRIP13 can be an effective target for the treatment of MM.[15,17] We also found that inhibition of TRIP13 could suppress the activation of NF-κB-dependent transcription.[15] Moreover, many studies indicate that the NF-κB pathway is widely involved in mediating the progression and drug resistance in MM.[34-36] Therefore, we hypothesized that TRIP13 could activate the NF-κB pathway in MM. In order to confirm this, we performed RNA-seq analysis and found that TRIP13 was positively correlated with the activation of NF-κB pathway. Moreover, results of immunoblotting and immunofluorescence suggested high expression of TRIP13 activated proteins involved in NF-κB signaling and an increase in the transfer of NF-κB p65 from cytoplasm to nucleus. In order to further investigate the specific mechanism of how TRIP13 activated the NF-κB pathway, we overlaid the list of proteins identified in the TRIP13 co-immunoprecipitation group from the LC-

MS/MS analysis. Of note, RPS3, a non-Rel subunit of NF-κB known to regulate several physiological processes, was first identified to interact with TRIP13 in our current study.

In order to understand the regulatory mechanism between TRIP13 and RPS3, we performed a series of *in vitro* experiments and found no effect on the expression of RPS3 regardless of whether TRIP13 was overexpressed or knocked down. Studies have shown that post-translational modifications play important roles in regulating the various extraribosomal functions of RPS3.[10] Specifically, the phosphorylation status of RPS3 can influence its binding function.[10,12] Here, we demonstrate for the first time that RPS3 is hyperphosphorylated at threonine residues when TRIP13 is overexpressed, and T221 on RPS3 is identified as a specific site that was affected by TRIP13. However, TRIP13 itself has no kinase activity. In line with previous reports that PKCδ could phosphorylate RPS3 at T221 site,[28,29] we observed that PKCδ was involved in the phosphorylation of RPS3 and the activation of NF-κB pathway in the context of TRIP13 overexpression. Additionally, selective inhibition of PKCδ could also overcome TRIP13-induced bortezomib resistance of MM. Overall, TRIP13 acts as a mediator through binding PKCδ and RPS3 to promote the phosphorylation activation of RPS3 by PKCδ, which further activates NF-κB signaling, including cell survival and drug resistance of MM (Figure 8). TRIP13 has been identified as an AAA-ATPase.[22-24] Currently, the detailed mechanisms underlying the regulation of the TRIP13-RPS3 axis, including the role of TRIP13 ATP hydrolysis and other potential factors, are the focus of ongoing studies in our laboratory.

We found that protein expression levels of TRIP13 and phosphorylated RPS3 in BR MM cells were significantly higher than that in bortezomib-sensitive ones. And we observed hyperactivation of the NF-κB pathway in drug-resistant cells.

It has been reported that MM cells hijack stromal cells to secrete cytokines to activate the NF-κB pathway, resulting in tumor growth and drug resistance.[37] In our previous study, DCZ0415 acted as a small molecule inhibitor that could target TRIP13 and induce cell death by inhibiting the NF-κB signaling pathway.[17] Intriguingly, we found in the current study that DCZ0415 significantly decreased levels of p-RPS3 in both MM cells and TRIP13-OE MM cells. Our previous paper demonstrated that the antimyeloma activity of DCZ0415 was dependent on TRIP13.[17] In the current study, we observed that the knockout of *RPS3* induced the loss of sensitivity MM cells to DCZ0415. Moreover, treatment of TRIP13-OE cells with DCZ0415 exhibited augmented cytotoxicity, while this effect was partially attenuated upon knockdown of RPS3. These findings indicate that DCZ0415 holds immense potential for drug-resistant MM, and the effects of DCZ0415 on drug-resistant cells is dependent on TRIP13-RPS3 axis. Our previous paper reported the antimyeloma activity of DCZ0415 in primary cells derived from drug-resistant patients with myeloma.[17] The findings in current study provide additional insights into the significant role of DCZ0415 in synergistically enhancing the efficacy of bortezomib in drug-resistant MM both *in vivo* and *in vitro*, providing the preclinical framework for combination clinical trials. Mechanically, DCZ0415 combined with bortezomib had a potent role in suppressing the activation of the NF-κB pathway.

In conclusion, our current studies have identified a novel role of TRIP13-PKCδ/PRS3 in consistently activating NF-κB during the development of resistance against proteasome inhibitor therapy in MM. This work raises the possibility and provides the first proof of concept in mouse models that targeting RPS3 in combination with the MM first-line therapeutic bortezomib may be a suitable way to overcome therapy resistance.[38]

Disclosures
No conflicts of interests to disclose.

Contributions
JS, GC, XG and WZ designed the experiments, analyzed data and prepared the manuscript. GC, XJ, YW, L-X, DY, SC, H-D, K-H, GW, B-L, ZX, YL, HW, T-Z, DS, G-Y and XW performed the experiments. All authors discussed the results and approved the final version of the manuscript.

Data-sharing statement
Original data is available by contacting the corresponding authors.

References

1. van de Donk N, Pawlyn C, Yong KL. Multiple myeloma. Lancet. 2021;397(10272):410-427.
2. Cowan AJ, Green DJ, Kwok M, et al. Diagnosis and management of multiple myeloma: a review. JAMA. 2022;327(5):464-477.
3. Nishida H. Rapid progress in immunotherapies for multiple myeloma: an updated comprehensive review. Cancers (Basel). 2021;13(11):4.
4. Podar K, Leleu X. Relapsed/refractory multiple myeloma in 2020/2021 and beyond. Cancers (Basel). 2021;13(20):5.
5. Alagpulinsa DA, Szalat RE, Poznansky MC, Shmookler Reis RJ. Genomic instability in multiple myeloma. Trends Cancer. 2020;6(10):858-873.
6. Neri P, Bahlis NJ. Genomic instability in multiple myeloma: mechanisms and therapeutic implications. Expert Opin Biol Ther. 2013;13(Suppl 1):S69-82.
7. Mitterer V, Murat G, Rety S, et al. Sequential domain assembly of ribosomal protein S3 drives 40S subunit maturation. Nat Commun. 2016;7:10336.
8. Lee SB, Kwon IS, Park J, et al. Ribosomal protein S3, a new substrate of Akt, serves as a signal mediator between neuronal apoptosis and DNA repair. J Biol Chem. 2010;285(38):29457-29468.
9. Gao X, Hardwidge PR. Ribosomal protein s3: a multifunctional target of attaching/effacing bacterial pathogens. Front Microbiol. 2011;2:137.
10. Graifer D, Malygin A, Zharkov DO, Karpova G. Eukaryotic ribosomal protein S3: a constituent of translational machinery and an extraribosomal player in various cellular processes. Biochimie. 2014;99:8-18.
11. Wan F, Anderson DE, Barnitz RA, et al. Ribosomal protein S3: a KH domain subunit in NF-kappaB complexes that mediates selective gene regulation. Cell. 2007;131(5):927-939.
12. Wan F, Lenardo MJ. The nuclear signaling of NF-kappaB: current knowledge, new insights, and future perspectives. Cell Res. 2010;20(1):24-33.
13. Wan F, Weaver A, Gao X, Bern M, Hardwidge PR, Lenardo MJ. IKKbeta phosphorylation regulates RPS3 nuclear translocation and NF-kappaB function during infection with Escherichia coli strain O157:H7. Nat Immunol. 2011;12(4):335-343.
14. Yang HJ, Youn H, Seong KM, Jin YW, Kim J, Youn B. Phosphorylation of ribosomal protein S3 and antiapoptotic TRAF2 protein mediates radioresistance in non-small cell lung cancer cells. J Biol Chem. 2013;288(5):2965-2975.
15. Tao Y, Yang G, Yang H, et al. TRIP13 impairs mitotic checkpoint surveillance and is associated with poor prognosis in multiple myeloma. Oncotarget. 2017;8(16):26718-26731.
16. Li C, Xia J, Franqui-Machin R, et al. TRIP13 modulates protein deubiquitination and accelerates tumor development and progression of B cell malignancies. J Clin Invest. 2021;131(14):e146893.
17. Wang Y, Huang J, Li B, et al. A small-molecule inhibitor targeting TRIP13 suppresses multiple myeloma progression. Cancer Res. 2020;80(3):536-548.
18. Lan J, Huang J, Tao X, et al. Evaluation of the TRIP13 level in

breast cancer and insights into potential molecular pathways. J Cell Mol Med. 2022;26(9):2673-2685.

19. Sheng N, Yan L, Wu K, et al. TRIP13 promotes tumor growth and is associated with poor prognosis in colorectal cancer. Cell Death Dis. 2018;9(3):402.

20. Li W, Zhang G, Li X, et al. Thyroid hormone receptor interactor 13 (TRIP13) overexpression associated with tumor progression and poor prognosis in lung adenocarcinoma. Biochem Biophys Res Commun. 2018;499(3):416-424.

21. Banerjee R, Russo N, Liu M, et al. TRIP13 promotes error-prone nonhomologous end joining and induces chemoresistance in head and neck cancer. Nat Commun. 2014;5:4527.

22. Alfieri C, Chang L, Barford D. Mechanism for remodelling of the cell cycle checkpoint protein MAD2 by the ATPase TRIP13. Nature. 2018;559(7713):274-278.

23. Ye Q, Rosenberg SC, Moeller A, Speir JA, Su TY, Corbett KD. TRIP13 is a protein-remodeling AAA+ ATPase that catalyzes MAD2 conformation switching. Elife. 2015;4:e07367.

24. Sarangi P, Clairmont CS, Galli LD, Moreau LA, D'Andrea AD. p31(comet) promotes homologous recombination by inactivating REV7 through the TRIP13 ATPase. Proc Natl Acad Sci U S A. 2020;117(43):26795-26803.

25. Hu L, Li B, Chen G, et al. A novel M phase blocker, DCZ3301 enhances the sensitivity of bortezomib in resistant multiple myeloma through DNA damage and mitotic catastrophe. J Exp Clin Cancer Res. 2020;39(1):105.

26. Xie Y, Wang Y, Xu Z, et al. Preclinical validation and phase I trial of 4-hydroxysalicylanilide, targeting ribonucleotide reductase mediated dNTP synthesis in multiple myeloma. J Biomed Sci. 2022;29(1):32.

27. Chen G, Hu K, Sun H, et al. A novel phosphoramide compound, DCZ0847, displays in vitro and in vivo anti-myeloma activity, alone or in combination with bortezomib. Cancer Lett.

2020;478:45-55.

28. Kim TS, Kim HD, Kim J. PKCdelta-dependent functional switch of rpS3 between translation and DNA repair. Biochim Biophys Acta. 2009;1793(2):395-405.

29. Kim TS, Kim HD, Shin HS, Kim J. Phosphorylation status of nuclear ribosomal protein S3 is reciprocally regulated by protein kinase Cdelta and protein phosphatase 2A. J Biol Chem. 2009;284(32):21201-21208.

30. Robak P, Drozdz I, Szemraj J, Robak T. Drug resistance in multiple myeloma. Cancer Treat Rev. 2018;70:199-208.

31. Nagao-Kitamoto H, Setoguchi T, Kitamoto S, et al. Ribosomal protein S3 regulates GLI2-mediated osteosarcoma invasion. Cancer Lett. 2015;356(2 Pt B):855-861.

32. Tian Y, Qin L, Qiu H, et al. RPS3 regulates melanoma cell growth and apoptosis by targeting Cyto C/Ca2+/MICU1 dependent mitochondrial signaling. Oncotarget. 2015;6(30):29614-29625.

33. Kim W, Youn H, Lee S, et al. RNF138-mediated ubiquitination of rpS3 is required for resistance of glioblastoma cells to radiation-induced apoptosis. Exp Mol Med. 2018;50(1):e434.

34. Baud V, Karin M. Is NF-kappaB a good target for cancer therapy? Hopes and pitfalls. Nat Rev Drug Discov. 2009;8(1):33-40.

35. Vrabel D, Pour L, Sevcikova S. The impact of NF-kappaB signaling on pathogenesis and current treatment strategies in multiple myeloma. Blood Rev. 2019;34:56-66.

36. Vo JN, Wu YM, Mishler J, et al. The genetic heterogeneity and drug resistance mechanisms of relapsed refractory multiple myeloma. Nat Commun. 2022;13(1):3750.

37. Fabre C, Mimura N, Bobb K, et al. Dual inhibition of canonical and noncanonical NF-kappaB pathways demonstrates significant antitumor activities in multiple myeloma. Clin Cancer Res. 2012;18(17):4669-4681.

38. Moreau P, Richardson PG, Cavo M, et al. Proteasome inhibitors in multiple myeloma: 10 years later. Blood. 2012;120(5):947-959.